Nanotechnology **20** (2009) 365503 (4pp) doi:10.1088/0957-4484/20/36/365503

Fast spiral-scan atomic force microscopy

I A Mahmood and S O Reza Moheimani

School of Electrical Engineering and Computer Science, The University of Newcastle, Callaghan, NSW 2308, Australia

E-mail: Reza.Moheimani@newcastle.edu.au

Received 23 April 2009, in final form 18 June 2009
Published 18 August 2009
Online at stacks.iop.org/Nano/20/365503

Abstract

In this paper, we describe a new scanning technique for fast atomic force microscopy. In this method, the sample is scanned in a spiral pattern instead of the well established raster pattern. A spiral scan can be produced by applying single frequency cosine and sine signals with slowly varying amplitudes to the x-axis and y-axis of an atomic force microscope (AFM) scanner respectively. The use of the single tone input signals allows the scanner to move at high speeds without exciting the mechanical resonance of the device and with relatively small control efforts. Experimental results obtained by implementing this technique on a commercial AFM indicate that high-quality images can be generated at scan frequencies well beyond the raster scans.

(Some figures in this article are in colour only in the electronic version)

1. Introduction

Atomic force microscope (AFM) was invented by Binnig *et al* in 1986 [1]. Since then, it has become an essential tool for nanotechnology research. The AFM is mainly used for imaging surface topographies and measuring surface forces of conducting as well as nonconducting samples with very high precision. The basic components of the AFM include a micro-cantilever with a sharp tip on one end, a scanner and a laser-photodetector sensor. During operations, the tip of the micro-cantilever is brought very close to the sample surface at a distance of the order of a few nanometers, or less. At such a distance, the interactive forces that exist between the tip and the sample surface change the static and dynamic deflections of the micro-cantilever. These deflections are detected by the laser-photodetector sensor and are used as a measurement to determine the interactive forces. These measurements can be used to generate the sample's surface topography or used as a feedback signal to keep the interactive force constant [2].

An AFM image of a sample is generated by scanning the tip over the entire surface of the sample that is to be imaged. In today's commercially available AFMs, the scanning is normally performed in a raster pattern. A raster pattern is attained by applying a triangular waveform to the fast axis (x-axis) and a staircase, or a very slow ramp signal to the slow axis (y-axis) of the scanner. In order to perform a high-speed raster scan for fast atomic force microscopy, a high frequency triangular waveform needs to be used. A drawback of a triangular waveform is that it contains all odd harmonics of the fundamental frequency whose amplitudes attenuate as $1/n^2$, with n being the harmonic number [3]. If a fast triangular waveform is applied to the scanner, it will inevitably excite the mechanical resonance of the scanner. Consequently, this causes the scanner to vibrate and trace a distorted triangular waveform along the x-axis which can significantly distort the generated image. To avoid this complication, the scanning speed of AFMs is often limited to about 10–100 times lower then the scanner's first resonance frequency [4]. Recently, there has been significant interest in utilizing feedback control to deal with the resonant nature of AFM nanopositioners, e.g. see [5] for an exhaustive overview of the literature, and [6–11] for further related results. In this approach, a feedback controller is used to flatten the frequency response of the scanner, thus allowing for faster scans. However, despite the significant improvement that can be achieved, the problem of tracking a fast triangular signal is inherently difficult due to the limited mechanical bandwidth of the device.

This paper proposes a new scanning technique for fast atomic force microscopy by forcing the scanner to follow a spiral trajectory illustrated in figure 1. This pattern is known as the Archimedean spiral. A property of this curve is that its pitch P, which is the distance between two consecutive intersections of the spiral curve with any line passing through the origin, is constant [12]. This property is quite important for scanning purposes as it ensures that the sample surface is scanned uniformly. The proposed method is

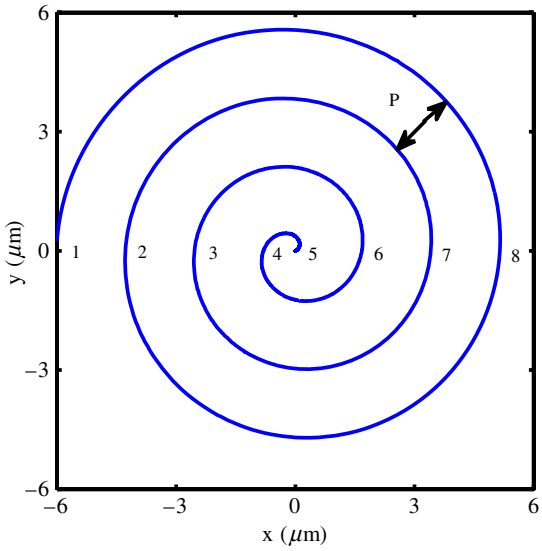

Figure 1. Spiral scan of 6 μm radius with number of curves = 8.

an alternative to raster-based sinusoidal scan methods that are used to achieve fast scans in e.g., scanning near-field optical microscopy (SNOM) [13]. In spiral scanning, both axes follow sinusoidal signals of identical frequencies resulting in a smooth trajectory. This avoids the transient behavior that may occur in sinusoidal scans as the probe moves from one line to the next. Furthermore the proposed method does not require specialized hardware, e.g. a tuning fork actuator, and can be implemented on a standard AFM with minor software modifications.

The paper is organized as follows. The generation of input signals to produce the spiral pattern is described in detail in section 2. Section 3 provides descriptions of the AFM and other experimental setups used in this work. In section 4 experimental results are presented to illustrate the improvement in imaging speed that can be achieved with the proposed new scan trajectory. Finally, section 5 concludes the paper.

2. Spiral scan

The equation that generates the spiral of pitch P and traced at an angular velocity of ω can be derived from a differential equation given in [14] as

$$\frac{\mathrm{d}r}{\mathrm{d}t} = \frac{P\omega}{2\pi} \tag{1}$$

where r is the instantaneous radius at time t. Equation (1) is solved for r by integrating both sides to obtain

$$r = \frac{P}{2\pi}\omega t \tag{2}$$

for $r = 0$ at $t = 0$. The pitch P is calculated as

$$P = \frac{\text{spiral radius} \times 2}{\text{number of curves} - 1} \tag{3}$$

where number of curves is defined as the number of times the spiral curve crosses through the line $y = 0$. The equation that

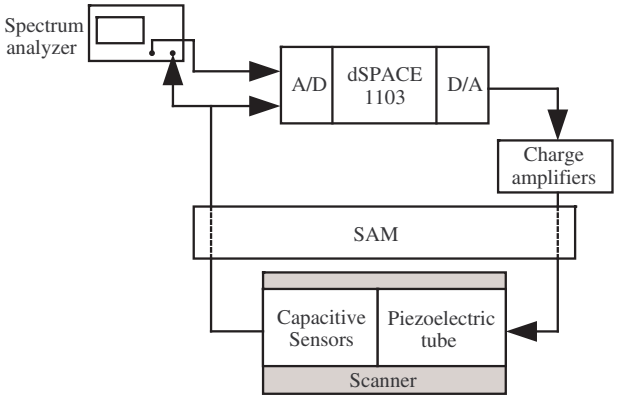

Figure 2. Block diagram of the experimental setup.

describes the total scan time t_{total} associated with a spiral scan can be derived by integrating both sides of equation (1) as

$$\int_{r_{\text{start}}}^{r_{\text{end}}} \mathrm{d}r = \frac{P\omega}{2\pi} \int_{t_{\text{start}}}^{t_{\text{end}}} \mathrm{d}t \tag{4}$$

where r_{start} and r_{end} are initial and final values of the spiral radius, and t_{start} and t_{end} are initial and final values of the scan time. From equation (4), if $r_{\text{start}} = 0$ at $t_{\text{start}} = 0$ and $t_{\text{total}} = t_{\text{end}} - t_{\text{start}}$, we obtain

$$t_{\text{total}} = \frac{2\pi r_{\text{end}}}{P\omega}. \tag{5}$$

In this work, the proposed spiral scan was implemented using a piezoelectric tube scanner. In order to move the scanner in a spiral trajectory, equation (2) is transformed into Cartesian coordinates. The transformed equations are

$$x_{\text{s}} = r\cos\theta \tag{6}$$

and

$$y_{\text{s}} = r\sin\theta \tag{7}$$

where x_{s} and y_{s} are input signals to be applied to the scanner in the x and y axes respectively and $\theta = \omega t$ is the angle. It can be inferred from (6) and (7) that, to move the scanner in a spiral trajectory, one only needs to apply slowly varying amplitude single frequency cosine and sine signals to the x- and y-axes of the scanner respectively. The use of the single frequency input signals allows the scanner to be moved at high speed without exciting the mechanical resonance of the scanner. Additionally, closed-loop tracking of these input signals requires smaller control efforts as compared to the tracking of the triangular waveform.

In the method proposed above, the probe's linear velocity varies as a function of its distance from the spiral's origin. If the probe is to trace a spiral at a constant linear velocity, as is required in many applications, then ω can be made to change as a function of r, to keep the linear velocity of the probe constant.

3. System description

An experimental setup as illustrated in figure 2 was put together in order to investigate the spiral-scan capability in

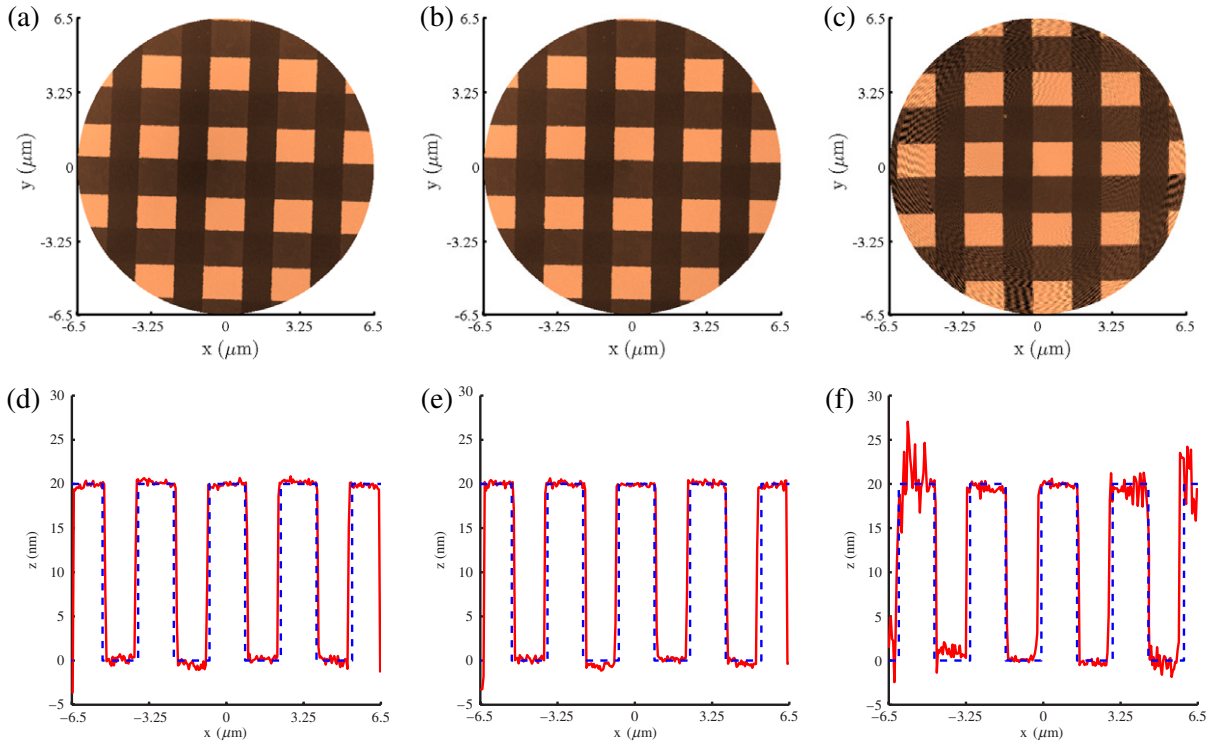

Figure 3. (a)–(c) AFM images of NT-MDT TGQ1 grating scanned in constant-height contact mode generated using CAV spiral for $f_s = 5, 30$ and 120 Hz (which corresponds to $\omega_s = 31.4$, 188.5 and 754.0 radians s^{-1}). The number of curves for these AFM images was set to 512. (d)–(f) The corresponding cross-section (solid) and reference (dash) curves of the AFM images illustrated in (a)–(c). The cross-section curves were taken about the center of the AFM images and parallel to the square profile of the calibration grating.

generating AFM images. The setup consisted of a commercial NT-MDT Ntegra scanning probe microscope (SPM) fitted with a closed-loop piezoelectric tube scanner. The scanner is incorporated with capacitive displacement sensors that provide measurements of the scanner's displacements in the x, y and z-axes. Two home made DC-accurate charge amplifiers [15] were used to drive the lateral axes of the piezoelectric tube scanner. A dSPACE-1103 rapid prototyping system was used to implement the feedback controllers in real time. The amplifiers and the SPM were interfaced with the dSPACE system using a signal access module (SAM) that allowed direct access to the scanner electrodes. This setup enabled us to directly control the lateral movements of the scanner.

Next, models of the scanner were identified for the purpose of controller design. Here, accurate models of the systems were obtained through the frequency domain subspace-based system identification approach described in [16]. It is worth mentioning that fairly accurate tracking of the spiral trajectory can be done in open-loop by shaping the input signals. However, closed-loop tracking was undertaken in this work in order to damp the first resonant mode of the piezoelectric tube scanner and to minimize effects such as hysteresis, creep and drift [17]. The overall control structure consists of an inner and an outer loop. The inner loop contains a second order positive position feedback (PPF) [18] controller that works to increase the overall damping of the scanner. The outer loop contains a high-gain integral controller to provide accurate tracking. The procedure that was followed to design these PPF controllers is well documented in [19]. Overall, the feedback controllers resulted in a high-bandwidth (540 Hz) closed-loop system.

4. Results

Having implemented the feedback controllers, we then moved on to investigate the spiral scanning capability in generating AFM images. The spiral scans were setup to produce images with $r_{end} = 6.5$ μm and number of curves $= 512$, i.e. the diameter of the resulting circular image consists of 512 pixels. A calibration grating NT-MDT TGQ1 with a 20 nm feature-height and a 3 μm period was used as an imaging sample. The AFM was setup to scan the sample in constant-height contact mode. During each scan, the probe deflection was measured and later used to construct AFM images of the sample topography. Figures 3(a)–(c) illustrate AFM images generated using the spiral scans with $\omega_s = 31.4$, 188.5 and 754.0 radians s^{-1}. These correspond to scanning frequencies of $f_s = 5, 30$ and 120 Hz respectively. Figures 3(d)–(f) illustrate the cross-section curves of these spiral scanned images at about $y = 0$ μm. The cross-section curves were taken in parallel to the square profile of the calibration grating. Note that, we used the probe deflection measurement of $f_s = 5$ Hz scan to calibrate the probe deflection measurements of other scan frequencies to the height of the calibration grating. This is possible because the probe deflection is very small and thus linear.

It can be observed from these figures that the obtained images are of a good quality and the lateral and vertical profiles

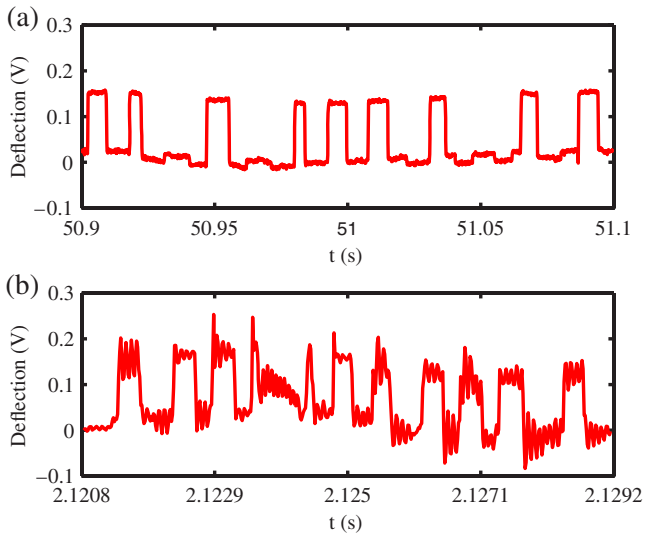

Figure 4. Probe deflection signals showing the profile of the calibration grating for (a) $f_s = 5$ Hz and (b) $f_s = 120$ Hz.

of the calibration grating are well captured. In particular, the images are free from typical distortions caused by tracking errors, scanner vibrations, hysteresis and creep. It is also worth mentioning that the area around the edges of the images was also well imaged. However, during high-speed scans with $\omega_s = 754.0$ radians s^{-1}, a wave-like artifact can be observed around the outer edges of the AFM images in figures 3(c) and (f). Upon a closer examination of the probe deflection signals, we found that the artifacts were a result of the excitation of the probe's resonance (≈12 kHz). Figure 4 illustrates the probe deflection signals between $r = 5.98$ and 6.00 μm for $f_s = 5$ and 120 Hz. Figure 4(a) shows that during a low-speed scan the probe deflection signal is free of vibrations. However at a high-speed scan, figure 4(b) shows that due to the existence of sharp corners in the topography of the sample, as the probe goes through a full circle, it faces step-like changes that tend to excite its first resonance frequency. This effect is much more profound when the sample is scanned at high frequencies. Thus, the image quality can be improved by using a stiffer micro-cantilever. This should allow for much higher scan frequencies.

5. Conclusions

In conclusion, in this paper we demonstrated how a spiral scans can be used to obtain AFM images. It is possible to achieve high-speed atomic force microscopy using spiral scanning, but other issues such as the vibrations in the AFM probe need to be considered and addressed. The possibility of using spiral scanning in other SPM applications such as STM should also be explored in the future.

References

[1] Binnig G, Quate C F and Gerber Ch 1986 Atomic force microscope *Phys. Rev. Lett.* **56** 930–3
[2] Bhushan B 2006 *Springer Handbook of Nanotechnology* (Berlin: Springer)
[3] Lathi B P 2004 *Linear Systems and Signals* 2nd edn (Oxford: Oxford University Press)
[4] Croft D, Shed G and Devasia S 2001 Creep, hysteresis, and vibration compensation for piezoactuators: atomic force microscopy application *ASME J. Dyn. Syst. Control* **123** 35–43
[5] Devasia S, Eleftheriou E and Moheimani S O R 2007 A survey of control issues in nanopositioning *IEEE Trans. Control Syst. Technol.* **15** 802–23
[6] Aphale S, Devasia S and Moheimani S O R 2008 High-bandwidth control of a piezoelectric nanopositioning stage in the presence of plant uncertainties *Nanotechnology* **19** 125503
[7] Bhikkaji B and Moheimani S O R 2008 Integral resonant control of a piezoelectric tube actuator for fast nano-scale positioning *IEEE/ASME Trans. Mechatronics* **13** 530–7
[8] Aphale S, Bhikkaji B and Moheimani S O R 2008 Minimizing scanning errors in piezoelectric stack-actuated nanopositioning platforms *IEEE Trans. Nanotechnol.* **7** 79–90
[9] Mahmood I A, Moheimani S O R and Liu K 2009 Tracking control of a nanopositioner using complementary sensors *IEEE Trans. Nanotechnol.* **8** 55–65
[10] Lee C and Salapaka S M 2009 Robust broadband nanopositioning: fundamental trade-offs, analysis, and design in a two-degree-of-freedom control framework *Nanotechnology* **20** 035501
[11] Stemmer A, Schitter G, Rieber J M and Allgower F 2005 Control strategies towards faster quantitative imaging in atomic force microscopy *Eur. J. Control* **11** 384–95
[12] Rutter J W 2000 *Geometry of Curves* (Boca Raton, FL: Chapman and Hall/CRC)
[13] Humphris A D L, Hobbs J K and Miles M 2003 Ultrahigh-speed scanning near-field optical microscopy capable of over 100 frames per second *Appl. Phys. Lett.* **83** 6–8
[14] Labinsky A N, Reynolds G A J and Halliday J 1993 A disk recording system and a method of controlling the rotation of a turn table in such a disk recording system *WO* 93/13524
[15] Fleming A J and Moheimani S O R 2006 Sensorless vibration suppression and scan compensation for piezoelectric tube nanopositioners *IEEE Trans. Control Syst. Technol.* **14** 33–44
[16] McKelvey T, Ackay H and Ljung L 1996 Subspace-based identification of infinite-dimensional multi-variable systems from frequency-response data *IEEE Trans. Autom. Control* **41** 960–79
[17] Moheimani S O R and Fleming A J 2006 *Piezoelectric Transducers for Vibration Control and Damping* (Berlin: Springer)
[18] Fanson J L and Caughey T K 1990 Positive position feedback-control for large space structures *AIAA J.* **28** 717–24
[19] Bhikkaji B, Ratnam M, Fleming A J and Moheimani S O R 2007 High-performance control of piezoelectric tube scanners *IEEE Trans. Control Syst. Technol.* **5** 853–66